Equatorwards breaking Rossby waves over the North Atlantic and Mediterranean region in the ECMWF operational Ensemble Prediction System

L. Wiegand[a,b]*and P. Knippertz[b]

[a] *Business unit 'Research and Development', German Weather Service, Offenbach am Main, Germany*

[b] *School of Earth and Environment, University of Leeds, Leeds, UK*

*Correspondence to: L. Wiegand, Deutscher Wetterdienst, Frankfurter Strasse 135, 63067 Offenbach am Main, Germany.

e-mail: lars.wiegand@dwd.de

The equatorward breaking of Rossby waves is a frequent feature of the synoptic-scale circulation over the North Atlantic. It often creates upper-level disturbances at low latitudes that can cause heavy precipitation in the Mediterranean region and Saharan dust outbreaks. The present study is the first to systematically explore the enormous dynamical information content of 12-years of data from the operational ensemble prediction system (EPS) of the European Centre for Medium-Range Weather Forecasts for this particular atmospheric feature. Dynamical precursors, forecast quality and predictability are investigated using a range of verification and analysis tools based on potential vorticity (PV). The main conclusions from this work are: (i) The EPS shows an underdispersive behaviour in the subtropics during PV streamer events. (ii) There is a tendency of too weak Rossby wave breaking and therefore a northward shift of the streamers in the forecast. (iii) Strong PV streamers in the medium-range forecasts are preceded by an active wave train in the subtropics, strongly positively titled PV anomalies in the extratropics and latent heating upstream of the PV streamer. There are no clear indications that blocking downstream is an important factor in contrast to other studies. Analysis tools developed specifically for EPS data in this study such as ensemble correlation techniques could be applied to other atmospheric phenomena in the future. **Copyright © 2012 Royal Meteorological Society**

Key Words: Ensemble prediction; Verification; Upper tropospheric dynamics; PV streamer; Diabatic processes; Atmospheric blocking, Ensemble correlation

Received . . .

Citation: . . .

1. Introduction

Rossby wave trains are the dominant dynamical feature of the upper troposphere in the mid-latitudes (e.g. Hoskins and Ambrizzi 1993). They usually propagate eastward with the mean flow, and their associated ridges and troughs are related to high- and low-pressure systems at the surface. In cases of non-linear amplification, Rossby wave breaking (RWB) can occur. The regions with the highest occurrence of RWB are at the downstream end of the storm tracks (Wernli and Sprenger 2007). Berggren *et al.* (1949) (reproduced by Rossby 1959) were among the first to show the propagation of a Rossby wave train over the North Atlantic, its amplification and the non-linear wave breaking. The fastest Rossby wave propagation is connected to the jet stream, which acts as a waveguide (Schwierz *et al.* 2004b) and coincides with the strongest isentropic gradients of potential vorticity (PV), which characterise the extratropical tropopause (Hoskins *et al.*

1985). RWB can result in elongated tongues of high-PV stratospheric air extending equatorwards and downwards into the troposphere, sometimes referred to as PV streamers. Using idealised modelling, Davies *et al.* (1991) and Thorncroft *et al.* (1993) demonstrate that PV streamers can form through dry dynamics as part of the life cycle of baroclinic waves. Diabatic heating can intensify the area of low PV upstream, which in turn can modify the development of some real-world PV streamers (Stoelinga 1996; Massacand *et al.* 2001). The diabatic heating is often associated with warm conveyor belts (WCBs), areas where warm and moist air is advected polewards ahead of the cold front of an extratropical cyclone (cf. e.g. Browning 1990; Carlson 1998). The air is then lifted into upper levels above the warm front, where it can either turn right or circulate around the centre of the cyclone. Climatological studies (e.g. Eckhardt *et al.* 2004) showed that the North Atlantic is a preferred region for WCB occurrence.

Furthermore, model sensitivity studies showed that downstream blocking over Europe can be crucial for a PV streamer penetration into low latitudes (Meier and Knippertz 2009). Atmospheric blocking involves a vertically coherent and quasi-stationary high pressure system in the extratropics, whose amplitude is large enough to disrupt the prevailing westerly circumpolar flow (Schwierz *et al.* 2004a). High-PV air arriving from the west can be forced to spread southward. According to Pelly and Hoskins (2003), the essence of atmospheric blocking is the poleward advection and subsequent cut-off of subtropical air induced by poleward RWB.

The number of northern hemispheric PV streamers peaks in summer (Postel and Hitchman 1999; Abatzoglou and Magnusdottir 2004; Wernli and Sprenger 2007). However, PV streamers that penetrate far into the subtropics mainly occur during boreal winter and spring and cluster over the central and eastern Pacific Ocean, and the eastern Atlantic Ocean and Mediterranean Sea (Kiladis and Weickmann 1997; Waugh and Polvani 2000; Froehlich and Knippertz 2008).

These subtropical PV streamers are often connected to high-impact weather events. Poleward moisture transport east of PV streamers can lead to heavy precipitation and flooding (e.g., Tripoli *et al.* 2005; Knippertz and Martin 2005, 2007). Studies for the European Alps (Massacand *et al.* 1998; Fehlmann *et al.* 2000; Hoinka and Davies 2007) have shown that heavy precipitation events are closely related to elongated stratospheric intrusions over western Europe, although not all PV streamers produce such events. Martius *et al.* (2006) found a link between longer-lived PV streamers and greater amounts of accumulated precipitation as well as a higher probability of intense precipitation events. At low latitudes PV streamers can trigger tropical convection (Kiladis and Weickmann 1992; Slingo 1998) as well as mid- and high-level pole- and eastward extending cloud bands from the Tropics into the subtropics denoted as Tropical Plumes (Iskenderian 1995; Knippertz 2005). Large-scale Saharan dust outbreaks are another significant meteorological phenomenon associated with PV streamers penetrating into the subtropics (Barkan *et al.* 2005; Slingo *et al.* 2006; Knippertz and Fink 2006). Thorncroft and Flocas (1997) found that PV anomalies arising ”naturally” during wave breaking can trigger cyclogenesis over the Sahara with high winds and low visibility along the cold front. PV streamers west of the Alps extending into Africa can initiate dust emission, transport and deposition on Alpine glaciers (Sodemann *et al.* 2006).

To the best of our knowledge this study is the first to investigate low-latitude PV streamers over the North Atlantic / Mediterranean region using ensemble predictions. The three main objectives of this study are: (i) to assess the accuracy of the forecasts with regard to position and intensity, and its dependance on lead-time; (ii) to assess predictability using the spread of the ensemble as an indicator; (iii) to investigate factors that control the penetration of PV streamers to low latitudes and how they influence the PV streamer forecasts.

Ensemble forecasts have been explored relatively little in dynamical research studies so far. For example Matsueda (2009) studied the predictability of atmospheric blocking events, while Froude (2010) concentrated on the prediction of

Table 1. Main changes to the ECMWF EPS during the study period 1997 to 2008. The abbreviations used in the table are: SV = singular vector; NH/SH = northern/southern hemisphere; TR = Tropics; Tx = triangular truncation at total wavenumber x; TLx = as Tx but with linear reduced Gaussian grid; HRes/VRes = horizontal/vertical resolution; Lx = vertical level; SP = stochastic physics.

Date	Characteristics of SVs			Forecast characteristics		
	HRes	VRes	Target Area	HRes	VRes	SP
Dec 1996	T42	L31	NH + SH	TL159	L31	No
Oct 1998	”	”	”	”	”	Yes
Oct 1999	”	L40	”	”	L40	”
Nov 2000	”	”	”	TL255	”	”
Jan 2002	”	”	NH + SH + TR	”	”	”
Feb 2006	”	L62	”	TL399	L62	”

extratropical cyclone tracks. Ensemble techniques were first operationally implemented in the 1990s, such that the data record is now long enough for a statistically meaningful investigation of specific weather systems. As the individual ensemble members start from initial conditions within the range of possible states of the atmosphere all forecasts are realistic realisations of possible evolutions. This allows an assessment of physical mechanisms and of predictability by quantifying the sensitivity to initial conditions. Several new diagnostic tools specifically designed for the analysis of ensemble data are developed and tested as part of this study.

The paper is structured as follows: Section 2 describes the data and methods. A climatology of PV streamers is discussed in section 3. Section 4 investigates the forecast performance including root-mean-square-error (RMSE)–spread comparisons, impacts of model changes and a discussion of spatial displacement errors. In section 5 an ensemble correlation analysis is presented to identify dynamical precursors. Conclusions are drawn in section 6.

2. Data & Method

This section describes the data used with a focus on the operational Ensemble Prediction System (EPS) of the European Centre for Medium-Range Weather Forecasts (ECMWF; section 2.1). Furthermore a method to identify PV streamers and its adaptation to EPS data is discussed (section 2.2).

2.1. ECMWF Ensemble Prediction System

The main data used in this study are forecasts from the EPS of the ECMWF. The EPS became operational in December 1992 with 33 members and one forecast per day at 1200 UTC using a spectral resolution of T63L19, i.e. truncation at wave number 63 (corresponds to ∼180 km grid spacing) and 19 vertical levels (Palmer *et al.* 1993; Molteni *et al.* 1996). One member, the so called control forecast, was initialised with the operational analysis. The remaining 32 members were calculated from perturbations applied to this analysis (Buizza *et al.* 1998; Barkmeijer *et al.* 1999). Buizza *et al.* (1998) found that increasing ensemble size and model resolution improve the ensemble skill. Therefore in December 1996 the operational system was upgraded to 51 members and resolution was increased to TL159L31. In order to avoid complications with comparing results based on different numbers of ensemble members, this study uses forecasts from the 12-year period January 1997 to December 2008 only. Although currently forecasts are started twice daily, only 1200 UTC data is used here in order to be compatible with the early part of the record. Lead-times of up to 10 days (240 hours) are investigated.

Table 1 summarises the main changes to the ECMWF EPS during this period (based on documentations available from the ECMWF website*). The horizontal resolution of the ensemble forecasts increased from TL159 to TL255 in November 2000 and to TL399 in February 2006, while the vertical resolution increased from L31 to L40 (October 1999) and then to L62 (February 2006). Within this study all fields are interpolated to a 2.5° by 2.5° latlon grid. At ECMWF perturbations to the operational analysis are calculated using the singular vector (SV) technique (Palmer *et al.* 1993). The horizontal resolution of SVs has remained T42 since the mid-1990s, but the vertical resolution increased from L31 to L40 in October 1999 and to L62 in February 2006. The optimisation time is 48 hours for the period considered here. Originally SVs were only computed for the northern and southern hemispheric extratropics poleward of 30°, but in January 2002 targeted moist SV calculations in the tropics have been added. To increase the ensemble spread by accounting for model errors, a 'stochastic physics' scheme was implemented in October 1998 (Buizza *et al.* 1998).

The changes to the operational system discussed above imply that the dataset analysed here is strictly speaking not homogeneous. This is clearly a limitation of this study and therefore some caution must be taken in interpreting statistics comprising the whole time period. Section 4.2, however, shows that the changes to the forecast quality are not necessarily monotonic with system updates, particularly not for longer lead-times. In addition, it should be noted that as long as there is no long-term comprehensive ensemble hindcast dataset using the operational EPS data is the only option for the kind of study presented here.

2.2. *PV Streamer Identification*

For the identification of significant upper-level disturbances at low-latitude, an adaptation of the algorithm described in Wernli and Sprenger (2007) is used, which is based on contours of isentropic PV equals 2 PVU (Potential Vorticity Unit, 1 PVU = $10^{-6}\,\mathrm{m^2 s^{-1} K kg^{-1}}$), a widely used definition of the dynamical tropopause (e.g. Appenzeller *et al.* 1996). On the synoptic scale the full Ertel PV is usually well approximated by the product of vertical stability and absolute vertical vorticity in pressure coordinates.

$$PV_p \cong -g\frac{\partial\Theta}{\partial p}\cdot(f+\xi), \tag{1}$$

where f is the Coriolis parameter, g the gravitational acceleration, ξ relative vorticity and Θ potential temperature with the latter two being a direct output from ECMWF model data. Until 2006 the ECMWF EPS data were only archived at five pressure levels (50, 200, 500, 700 and 925 hPa). Consequently, upper-level PV has to be approximated by the rather crude formulation below involving the 200 and 500 hPa levels only:

$$UPV \cong -g\frac{\partial\Theta}{\partial p}\cdot(f+\overline{\xi_p}) \cong -g\frac{\Theta_{500}-\Theta_{200}}{300hPa}\cdot(f+\frac{\xi_{500}+\xi_{200}}{2}) \tag{2}$$

A comparison between UPV and PV using all currently available ECMWF model levels shows generally similar geographical structures but somewhat smaller absolute values (not shown). This suggests that the rather simplified parameter UPV can be used for PV streamer identification, if adequate adaptions are applied.

The algorithm by Wernli and Sprenger (2007) checks for every pair of contour points whether the spherical distance between the two points d is smaller than a threshold D = 800 km while the distance along the contour l is larger than a threshold value L = 1500 km (cf. Figure 1 in Wernli and Sprenger 2007). If both criteria are fulfilled, the area bordered by

*http://www.ecmwf.int/products/data/technical/model_id/index.html, 03 February 2011

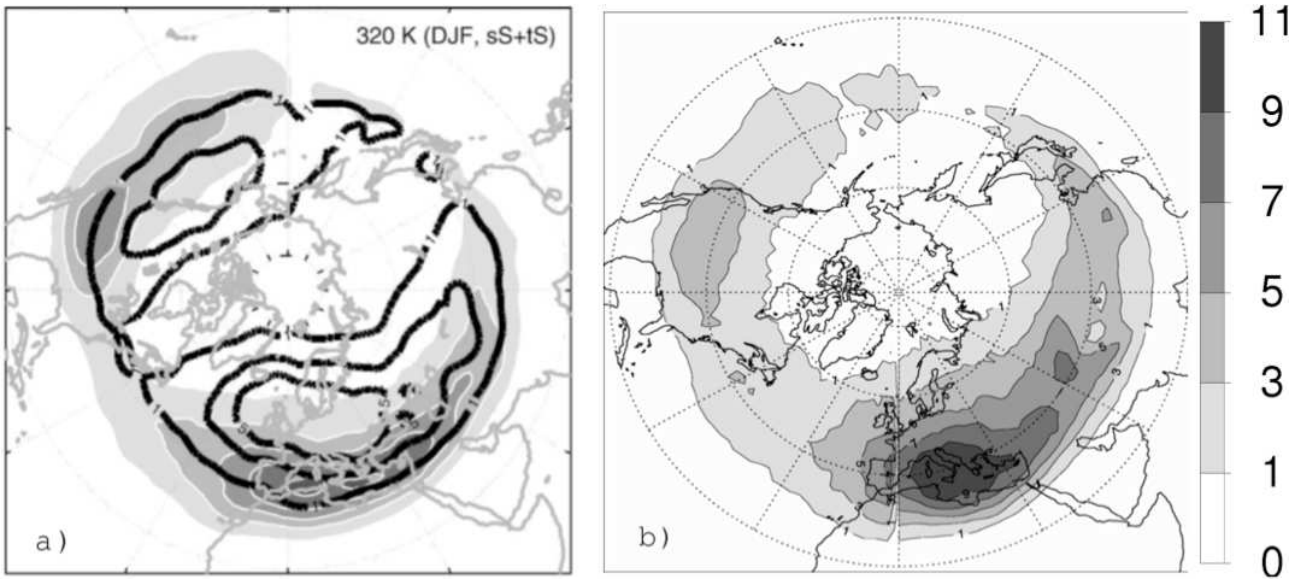

Figure 1. Winter mean (DJF) frequency of PV streamers in % (gray shading). (a) Taken from Wernli and Sprenger (2007) using PV on 320 K for the ERA-15 time period 1979–1993 (black solid lines are frequencies of PV cut-offs not relevant to this study) and (b) using UPV from the operational analysis during the study period 1997–2008.

this part of the contour line and the spherical line between the two points is defined as the PV streamer. To account for the systematically lower UPV compared to full PV, 1.5 PVU was used instead of 2 PVU.

Figure 1 shows a comparison between the original results from Wernli and Sprenger (2007) based on ECMWF ERA-15 re-analysis and the adapted algorithm using UPV calculated from twice daily operational analysis over the study period of this paper (1997–2008) for the winter months December to February. Absolute numbers and geographical distribution agree well, despite the differences in time period and identification algorithm. Maximum frequencies are found over the Mediterranean Sea stretching into adjacent Europe, Africa and Asia. A secondary maximum occurs over North America stretching into the adjacent North Pacific and Atlantic Oceans.

These results are used for detecting suitable PV streamer episodes to study EPS forecast performance using a simple tracking algorithm searching for spatial overlap of PV streamers during consecutive 12 or 24 hour time steps (i.e. one analysis time with no identified streamer is tolerated). An episode must consist of at least two identified streamers. Within a given episode the southernmost PV streamer point is required to be to the south of 27.5°N and between 30°W and 30°E meridionally (solid box in Figure 2) to filter out streamers with extreme equatorward extensions. This procedure identified 101 episodes, 52 of which were merged due to close proximity in time, ultimately giving 75 sufficiently independent episodes. One analysis time out of each episode was then subjectively selected as a verification time for the EPS analysis based on the following criteria: (i) southernmost extension, (ii) highest intensity, (iii) largest extension, (iv) highest impact on weather, e.g. precipitation and or dust mobilisation.

Figure 2 shows an example episode in February 1998, which was characterised by a high-amplitude ridge over central Europe and an anticyclonic wave breaking downstream. The strongly positively tilted PV streamer that formed from this RWB (marked with thick black lines) slowly moved from the Mediterranean Sea (Figure 2a) into northeastern Africa within the two days shown. Despite the clear connection to the previous and subsequent times, the algorithm fails to identify the streamer at 0000 UTC 19 February (2b), which is mainly due to the widening of the 1.5-PVU contour over Turkey. The deepest PV intrusion took place at 0000 UTC 20 February (Figure 2d), but as this time step is not available in the EPS data, the previous 1200 UTC 19 February 1998 (Figure 2c) was selected as verification date.

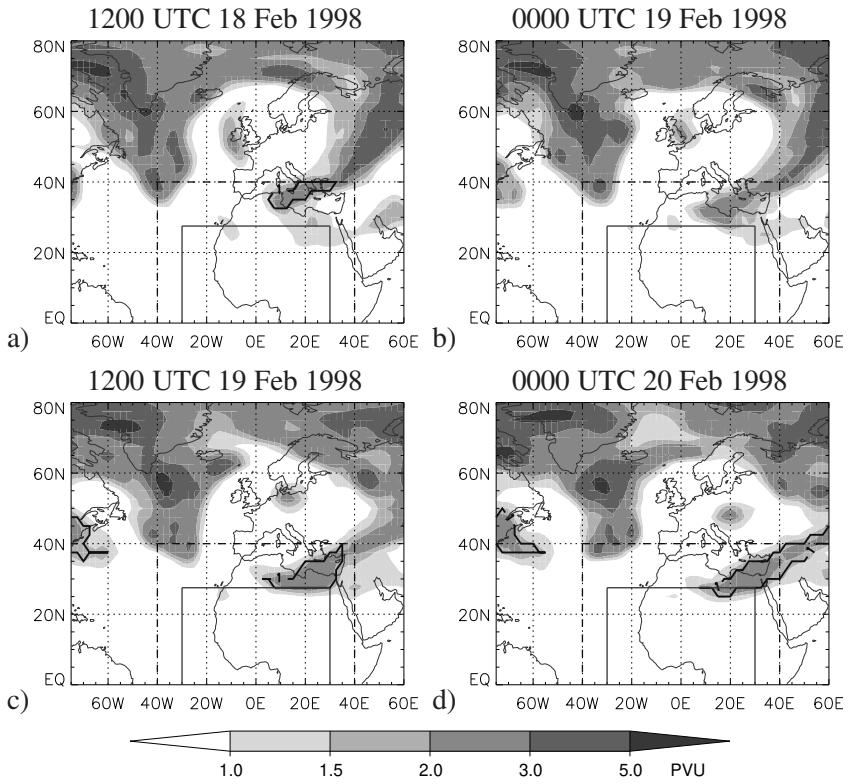

Figure 2. Example PV streamer episode from 1200 UTC 18 (a) to 0000 UTC 20 February 1998 (d). The shading is UPV in PVU. Thick black lines: Identified PV streamer contours (Identification done with an adapted algorithm from Wernli and Sprenger (2007). For details see text.); black solid rectangle: area that PV streamer need to reach during an episode to be considered for this study (0° - 27.5°N, 30°W - 30°E); black dashed rectangle: GFB used for verification as defined in section 2.3.

2.3. Verification methods

Different methods are used to verify the forecast performance of the ECMWF EPS. These are mainly based on simple RMSE calculations using UPV and 500 hPa geopotential height. A larger geographically fixed box (referred to as GFB and SRB from now on) and a smaller system-relative box (SRB) are used for the computations. The former borders 40°N – 0°S and 40°W – 40°E and covers the eastern Atlantic, southern Mediterranean Sea and northern hemispheric Africa (cf. dashed rectangle in Figure 2). The latter is only fixed in the northern and southern borders (40°N and 25°N), while the fixed east – west dimension of 25° is centred on the longitude where the box contains the maximum number of streamer grid points. Only central longitudes between 30°W and 30°E are considered. The SRB is used in sections 4.3 and 5. In addition, the actual streamer area (bordered by thick black lines in Figure 2) within GFB is used in section 4.1.

3. Climatology

Figure 3a shows the interannual distribution of the 75 cases identified in section 2.2 for the years 1997 to 2008. Averaged over the 12 years 6.25 PV streamers occur per year, varying from four (2000, 2003 and 2004) to nine (1999 and 2008). There is no clear trend or periodicity in this rather short time series. As expected low-latitude streamer activity is confined to boreal winter and spring from November to April (Figure 3b). Maximum total numbers of 24 occur in January corresponding to 2 on average per year. The annual cycle is mainly due to seasonal variations of temperature in the extratropics and the associated shift of the tropopause, and consequently the North Atlantic storm track. This distribution is consistent with various other studies as discussed in section 1 (Froehlich and Knippertz 2008, e.g.).

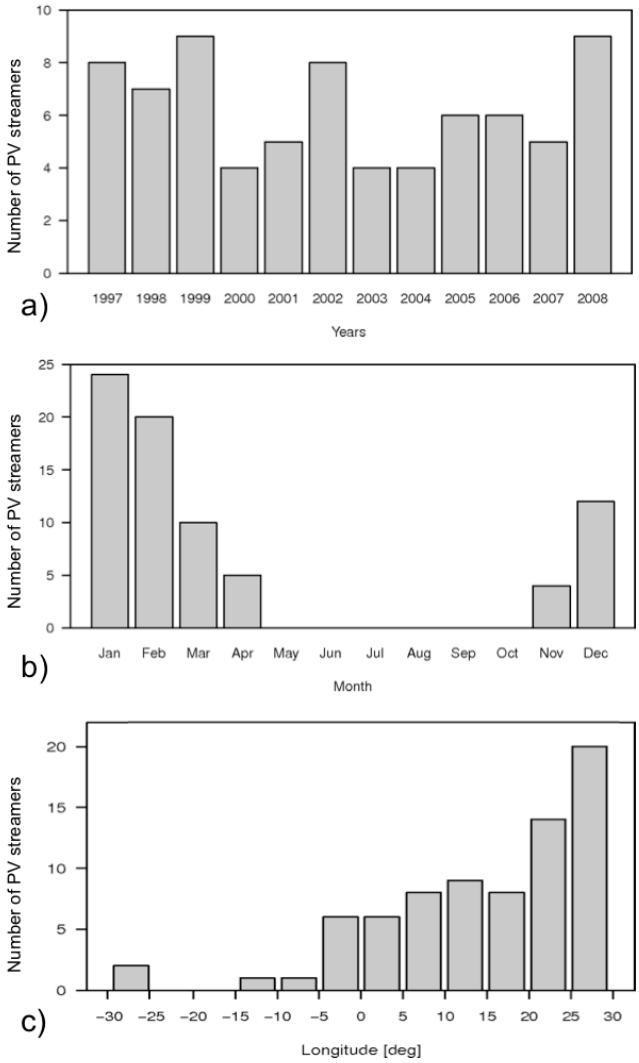

Figure 3. Number of PV streamers per a) year, b) month and c) longitude in 5° steps from 30°W - 30°E identified in ECMWF operational analysis data. The identification of the PV streamers is described in detail in section 2.2.

The distribution of the streamer position, defined as the centre longitude of SRB (see details in section 2.3), for all 75 PV streamer cases in 5° longitudinal steps shows a clear increase from west to east (Figure 3c), consistent with the horizontal distribution shown in Figure 1b. The maximum is found over the western half of Egypt (between 25°E and 30°E) with 20 cases over the twelve years examined. Together with neighbouring eastern Libya (20°E to 25°E), which has 14 cases, nearly half of all PV streamers under study are placed within this 10° longitudinal zone. The rest of the cases, except for two Atlantic streamers, are identified between the west coast of Morocco ($\sim$ 15°W) and the Gulf of Sidra (20°E) with the majority falling to the east of the Strait of Gibraltar. The two outliers over the Atlantic are both located at $\sim$ 30°W.

4. Forecast performance

4.1. RMSE-spread comparison

A well-configured EPS should be non-dispersive. A widely used indicator for this is that the RMSE of the ensemble mean is of a magnitude similar to the spread (standard deviation of member forecasts) (Leutbecher and Palmer 2008). A smaller (larger) spread is called underdispersive (overdispersive) behaviour.

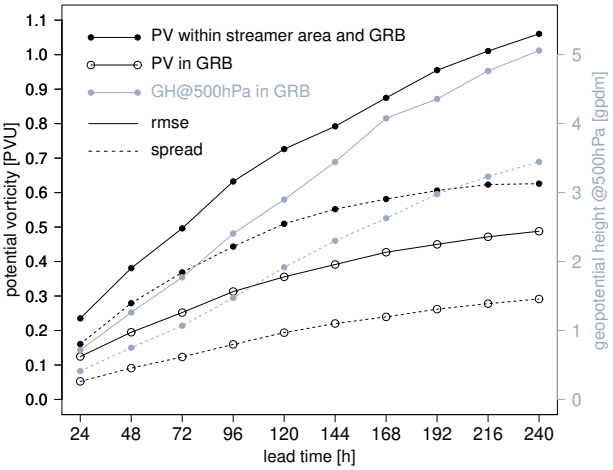

Figure 4. Comparison of RMSE (solid lines) and spread (dashed lines) for the 1- to 10- day ECMWF ensemble forecasts. RMSE and spread were averaged over 75 PV streamer cases and calculated for the PV (black lines with open circles) in GFB (defined in section 2.3), PV restricted to the PV streamer area within GFB (black lines with filled circles) and geopotential height at 500 hPa in GFB (grey lines).

Such a comparison, averaged over all 75 PV streamer cases, is shown in Figure 4 using UPV and 500 hPa geopotential height in the GFB as well as the area of the analysed PV streamer within the GFB as explained in section 2.3. In all three cases the RMSE and spread grow with lead time as expected. The overall behaviour is strongly underdispersive. Wiegand *et al.* (2011) studied a PV streamer case in May 2008 and found this underdispersive behaviour in all EPS within the TIGGE archive. The RMSE and spread values for UPV in the PV streamer area are nearly twice as large as those for UPV in GFB and keep increasing almost linearly for longer lead-times. The main reason for this behaviour is the generally low UPV south of 40°N (northern border of GFB), implying that the streamer constitutes a large anomaly. For grid points away from the PV streamer the differences between the forecast and the analysis are generally small, independent of the quality of the forecast, leading to lower spatially averaged values in a larger box. The continued growth of RMSE for UPV in the analysed PV streamer area implies considerable differences in location and or intensity at longer lead-times, although the sharp gradients at the edges of PV streamers can cause large RMSE, even for relatively minor spatial shifts already. To further investigate this, GFB values based on 500 hPa geopotential height, which is used by the majority of studies on EPS evaluation (Buizza *et al.* 2005, e.g.), are shown. Due to the continuous nature of geopotential height fields RMSE and spread keep growing more linearly with lead time than for UPV and therefore show a behaviour more similar to the UPV within the analysed PV streamer area values. The stronger increase of spread at long lead-times suggests less underdispersive behaviour than the UPV diagnostics.

4.2. Impacts of model changes

This section focuses on an investigation of changes in EPS performance for low-latitude PV streamers with changes to the operational forecasting system (e.g. resolution, singular vectors etc., see Table 1 for details).

Figure 5 shows RMSE and spread calculations using the GFB for six consecutive periods bordered by major model changes. The legend shows that the number of PV streamers identified in each period varies from 5 to 25. Therefore particularly the two middle periods with 5 and 6 identified systems, respectively, should be regarded with some caution. For short lead-times (24 h to 72 h) there is a clear decrease in RMSE for later model versions, particularly associated

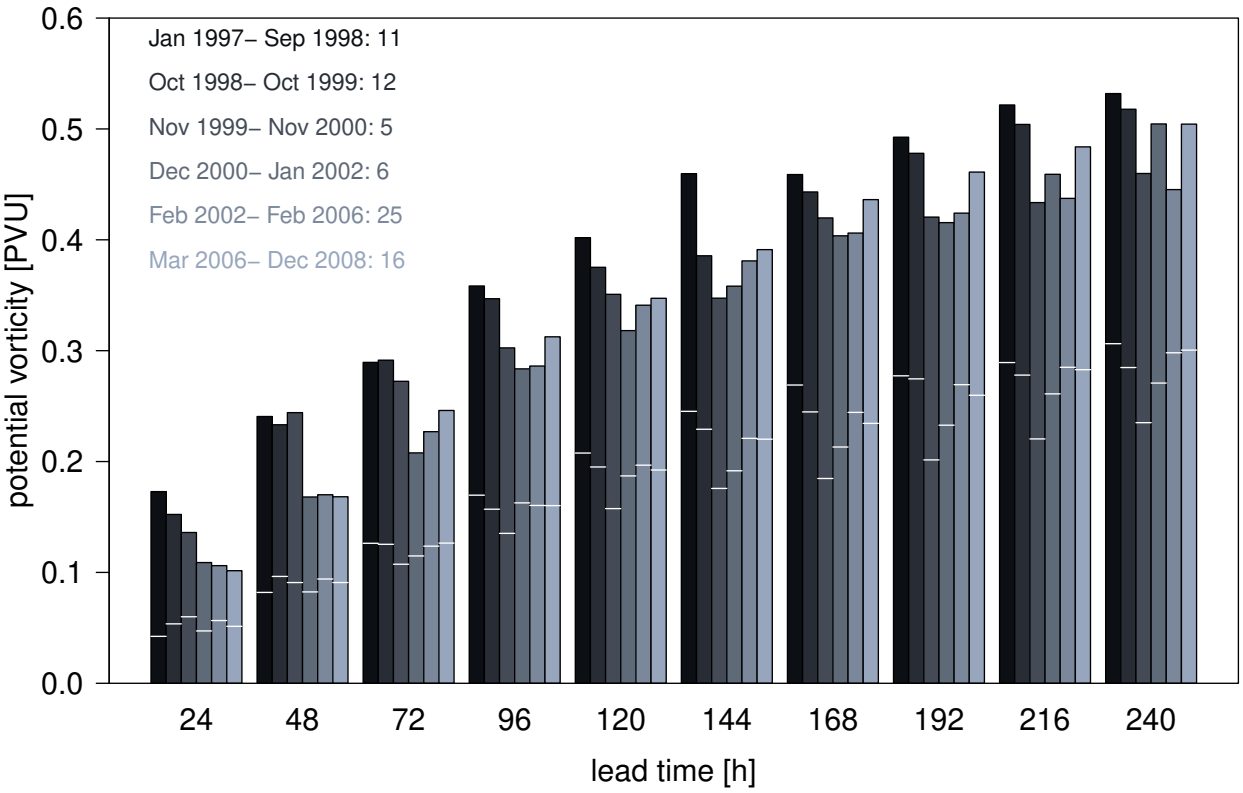

Figure 5. Comparison of RMSE (bars) and spread (white lines within bars) for the 1- to 10- day ECMWF ensemble forecasts separated into temporal sections based on EPS changes with time (Table 1). RMSE and spread were averaged over all 75 PV streamer cases and over the GFB (as black lines with open circles in Figure 4).

with the increase in horizontal resolution to TL255 in November 2000. The spread for these lead-times remains almost constant, leading to a considerable improvement of the underdispersive behaviour of the EPS. For longer lead-times the earliest period (January 1997 to October 1998) remains the poorest forecast and a general improvement with model version is evident, although not strictly monotonic. The changes in spread are more varied with a notable marked drop in the November 1999 to November 2000 period. lmprovements to the underdispersive behaviour at long lead-times are small. The introduction of stochastic physics in October 1998 does not show a clear increase for our analysis, but the introduction of tropical SVs in January 2002 does.

4.3. Displacement errors

To study a possible displacement error in the PV streamer forecasts, the SRB as defined in section 2.3 is shifted in steps of 2.5° over the forecast field in all four directions before differences in box averaged UPV to the verifying analysis are calculated. Figure 6 shows the results for four different lead-times. Squares stand for higher/lower averaged PV values inside the shifted box than in the analysis. The PV streamer is predicted correctly in terms of averaged UPV if there is no square. The squares in the middle of each plot show differences without any shifting. These grow with lead-time, reflecting the general increase of forecast error evident from Figure 4. For 24 h the smallest square is in the centre of the plot (Figure 6a), indicating accuracy in position and amplitude. Northward shifts of the SRB in the forecasts lead to slightly higher values, while southward shifts lead to dramatically lower values. This is to be expected from the low background values in the subtropics, where the streamers constitutes a large anomaly. Interestingly, there is a small east–west asymmetry

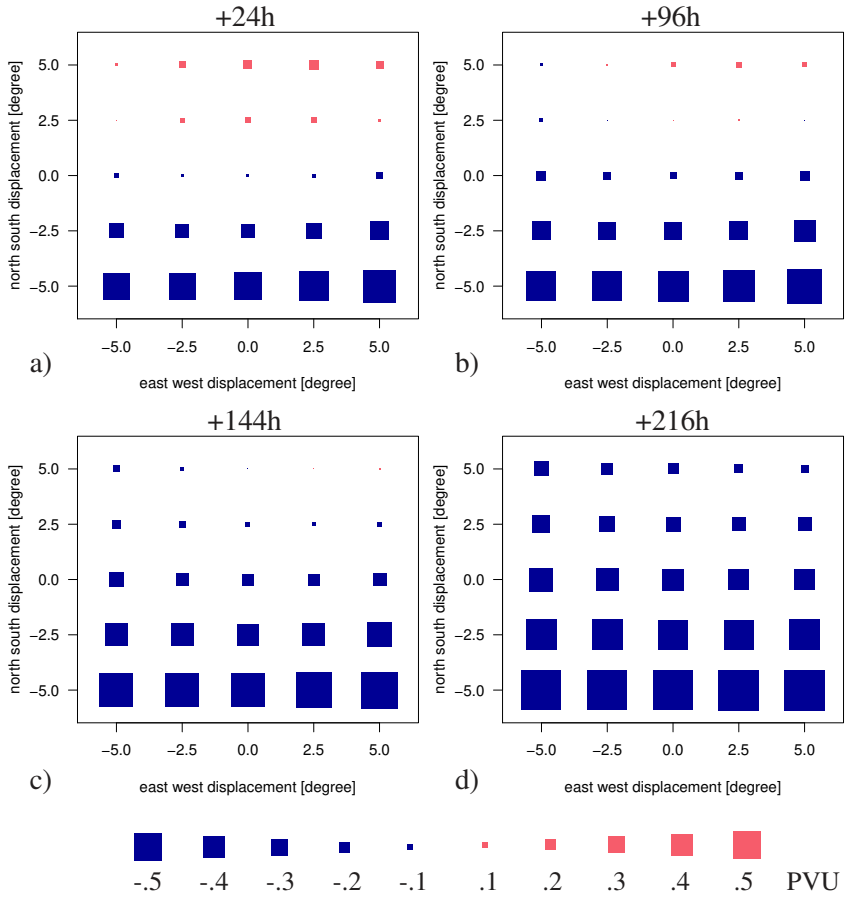

Figure 6. Analysis of displacement errors. Difference between SRB averaged UPV of displaced forecast fields and analysis fields for all 75 PV streamer events. The figures show the results for lead-times of (a) 24 h, (b) 96 h, 144 h and (d) 216 h.

that suggests a slight tendency for eastward displacement in the forecasts. For the longer lead-times there is a general shift to more blue colours indicating a weakening of the streamers in the forecasts (Figures 6b–d). At the same time the east–west asymmetry grows, eventually indicating lowest differences for boxes shifted by 5 degrees to the north and east in the forecasts. This suggests too weak RWB and too little penetration of the typically positively tilted streamers into low latitudes.

5. Ensemble Correlation Analysis

This section focuses on the identification of dynamical precursors for PV streamers over Africa using an ensemble correlation approach. Following previous work the analysis will concentrate on Rossby wave amplification, downstream blocking and diabatic heating upstream. The method will be explained in section 5.1 followed by an example case study in section 5.2 and a statistical analysis in section 5.3.

5.1. Method

The ensemble correlation method is adapted from Hawblitzel *et al.* (2007) who used correlations between different forecast variables to investigate precursors for successful predictions of convective systems. Here, the linear correlation between different forecast variables is investigated in the following way:

$$r\left(x_{i,j}^{t}, PV_{SRB}^{168h}\right) = \frac{\frac{1}{N-1}\sum_{n=1}^{N}\left({}^{n}x_{i,j}^{t} - \overline{x_{i,j}^{t}}\right)\left({}^{n}PV_{SRB}^{168h} - \overline{PV_{SRB}^{168h}}\right)}{\left[\frac{1}{N-1}\sum_{n=1}^{N}\left({}^{n}x_{i,j}^{t} - \overline{x_{i,j}^{t}}\right)^{2}\right]^{\frac{1}{2}}\left[\frac{1}{N-1}\sum_{n=1}^{N}\left({}^{n}PV_{SRB}^{168h} - \overline{PV_{SRB}^{168h}}\right)^{2}\right]^{\frac{1}{2}}} \tag{3}$$

The first key variable is ${}^{n}PV_{SRB}^{168h}$. It denotes the 168 hour forecast of UPV from the nth EPS member averaged over the SRB as defined in section 2.3 for one of the identified streamers. A 7-day lead time was chosen to give the ensemble enough time to spread significantly to ensure stable correlations. The second variable $x_{i,j}^{t}$ is the forecast of an atmospheric variable x at grid point i, j from the same nth member at an earlier lead-time t. The correlation is computed over all $N = 50$ EPS members.

As an example ${}^{Z200}r_{i,j}^{48h}$ is described hereafter to point out the essence of the correlation approach. Areas where this correlation is positive imply that ensemble members have a relatively high geopotential height at 200 hPa (Z200) at a given grid point i, j 48 hours into the forecast will develop a stronger PV streamer until the verification time, i.e. higher SRB-averaged UPV at 168 hours. Negative correlations indicate the opposite behaviour. This way dynamic precursors for particularly strong streamer developments can be extracted from a set of realistic realisations of the full non-linear evolution of the atmosphere, although, of course, correlation does not necessarily imply a causal relationship. Note that the amplitude of the correlation will be somewhat sensitive to the ensemble spread in PV_{SRB}^{168h}. Ensemble correlations were computed for all 75 identified PV streamers, for lead times of 48, 72, 96, 120, 144 and 168 hours and for the atmospheric variables UPV, geopotential height at 200 hPa (Z200), equivalent potential temperature at 850 hPa (THE850) and vertical wind at 700 hPa (w700). While the former is considered to detect wave amplification and blocking, the latter two give indications for upstream latent heating.

5.2. *Example Case*

Figure 7 shows the example streamer episode of 0000 UTC 01 December 2005, which nicely illustrates some of the main aspects of the ensemble correlation approach. Initialisation time for this case is 0000 UTC 24 November 2005.

The black lines in all panels of Figure 7 show UPV contours of 1.5 PVU taken from ECMWF analysis for better orientation. They show that the PV streamer over northwestern Africa forms from the zonal compression of a broad, almost stationary, high-amplitude ridge / trough pattern over the North Atlantic / western Europe associated with the approach of a short-wave trough, which moves from around Newfoundland into the central North Atlantic during the last four days of the development. There are indications for a northward cyclonic wave breaking over the North Atlantic during 30 November and 01 December 2005.

Let us begin the discussion of the ensemble correlations with the evolution at 200 hPa (top row). On 26 November (48 hours into the forecast) ensemble members that ultimately develop the strongest PV streamers are characterised by a wave train pattern in the subtropics with a broad ridge (2 maxima, marked as A) over the North Atlantic, a trough over southwest Europe / northwest Africa (B) and a ridge over northeast Africa (C), while signals at northern latitudes are generally weaker. On 27 November (72 hours into the forecast) the subtropical wave pattern is still clearly discernible, now with a highly negative signal over the east coast of North America (E) and a narrower ridge over the subtropical Atlantic (A*). In addition there is now also a strong signal at higher latitudes (A). While the analysed UPV contours suggest a cyclonic wave breaking over the northeastern Atlantic, the ensemble correlations indicate that ensemble members with the strongest PV streamers at 168 h develop a stronger northeastward tilt of the ridge (A+). From +96 h onwards the

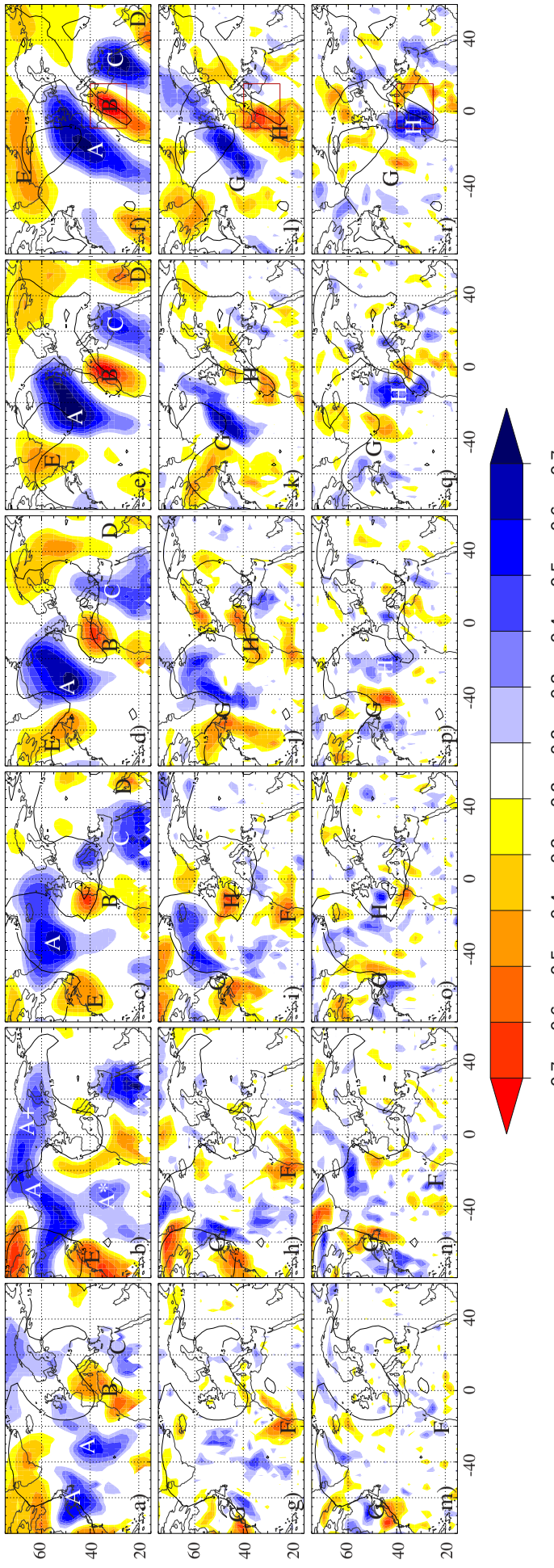

Figure 7. Example case for the ensemble correlation approach. Linear correlation coefficients are shown in colours. Correlated atmospheric variables are (i) geopotential height at 200 hPa (top), (ii) equivalent potential temperature at 850 hPa (middle) and (iii) vertical wind at 700 hPa (in pressure coordinates, so negative values correspond to rising) (bottom). Columns vary in forecast time from 48 h (left) to 168 h (right) in steps of 24 h (showing 0000 UTC 26 November 2005 to 0000 UTC 01 December 2005). Correlations above 0.23 are statistical significant at the 95% level, assuming independence for each ensemble member. Black lines depict corresponding UPV contours of 1.5 PVU taken from ECMWF analysis for better orientation. The box over which UPV is averaged at 168 hPa is shown in red in the right panels.

subtropical wave pattern is mainly confined to Africa with a trough over the western coast (B), a strong and persistent ridge over northeastern Africa (C), which might have contributed to the streamer intensification by blocking the westerly flow in the subtropics, and another trough over the Arabian Peninsula (D), while strongest signals are now generally found in the extratropics. Correlations between +96 and +144 h consistently indicate that members that ultimately develop the most intense streamers are characterised by (i) a slower moving and more southward extended trough over the western North Atlantic (E), (ii) a stronger and more positively tilted ridge over the central North Atlantic (A) and (iii) a narrower and more intense trough downstream (B). By the final time +168 h the correlation shows no separation between subtropical and extratropical wave activity anymore. The pattern generally has a strong positive tilt indicative of intense wave energy flux towards low latitude. The signal around the PV streamer indicates a higher intensity (by construction), but also an even more pronounced southward extent.

The middle and bottom panels in Figure 7 show the analogous correlations for THE850 and w700 to identify areas, where latent heating might influence the evolution of the wave in PV. Not surprisingly, the patterns are noisier than for Z200 and therefore the discussion will be confined to the few strongest and most coherent signals. In the early stages the subtropical wave seen in the Z200 plots creates a distinct anomaly of low THE850 air (cooler and/or drier) near the West African coast, associated with stronger northerlies and weak subsidence (marked as F in both bottom panels). The most coherent feature is the dipole of low THE850 / subsidence and high THE850 / ascent associated with the trough over the western North Atlantic from +72 h to +144 h (G). The slight upstream shift with respect to the Z200 signal (A) strongly suggests that latent heating in the region of a poleward transport of warm moist air contributes to an intensification of the downstream ridge, which helps to suppress the cyclonic wave breaking seen in the analysis and fosters dispersion of wave energy towards low latitudes as discussed above. During the last four days, an area of subsidence and low THE850 (H) develops underneath and to the west of the actual PV streamer. This is an indication of a stronger circulation, but at the same time could also help the streamer to survive longer due to less diabatic PV reduction in the drier air.

To further illustrate the correlation approach, Figure 8 provides a detailed look into two selected member forecasts (no. 22 and 10) and the corresponding analysis fields for THE850 at 0000 UTC on 28 November 2005 (corresponds to +96 h forecasts; left) and UPV at the verification time, i.e. 0000 UTC 01 December 2005 (corresponds to +168 h forecasts; right). The selected members are chosen according to their UPV averaged over SRB with member 22 (10) having one of the highest (lowest) values among all EPS members. The THE850 analysis (Figure 8a) four days before verification time reveals a high-amplitude trough-ridge-trough-ridge pattern covering the North Atlantic and adjacent continents. Very high THE850 values of more than 306 K reach Greenland in the distinctive ridge over the western North Atlantic. The two 96 h forecasts match the general pattern reasonably well (Figures 8c and e). The most striking differences are generally lower THE850 values in the high-latitude troughs, a weaker ridge over the western North Atlantic, but higher values in the subtropics around 40°W. Member 10 shows indications of a more cyclonic wave breaking and an advection of the tongue of high THE850 away from Greenland (Figure 8e).

The right panels in Figure 8 depict the corresponding UPV fields four days later. The analysis (Figure 8b) shows the extremely elongated and narrow PV streamer stretching from central Europe and the Mediterranean Sea into the Sahara as discussed in the context of Figure 7. EPS member 22 predicts the PV streamer in fairly good agreement with the analysis, but a little wider, less extended towards the south and with slightly higher values in the tip (Figure 8d). Other features of the UPV distribution, however, are less well matched, for example the large deviations over Scandinavia and Canada. On

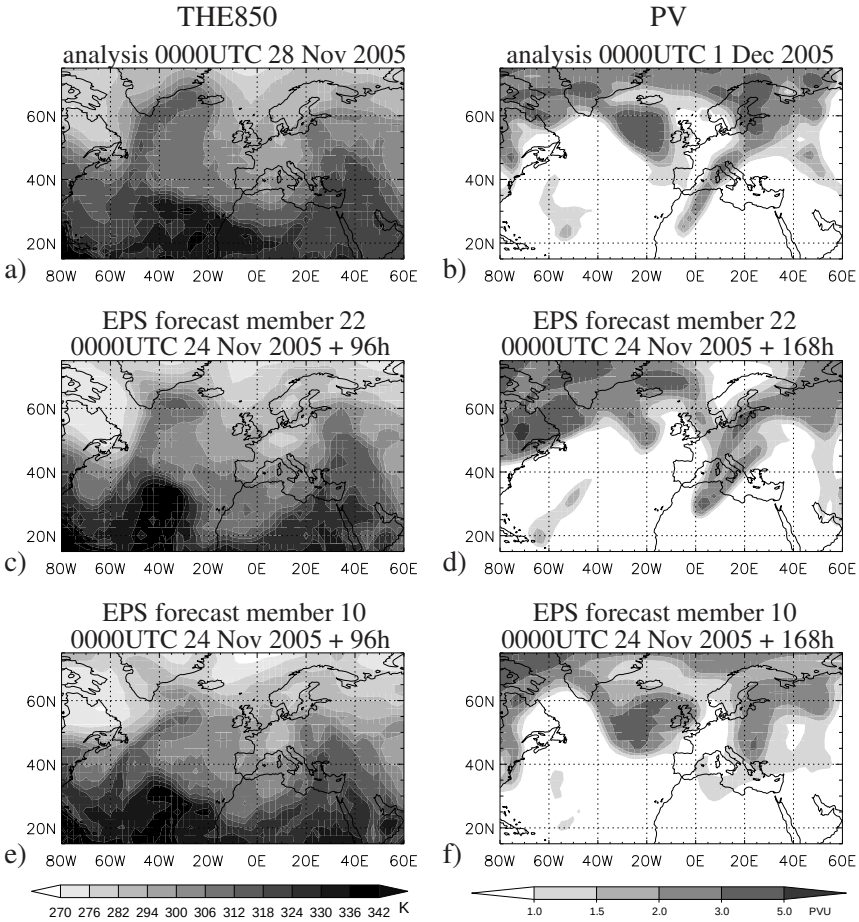

Figure 8. Comparison of equivalent potential temperature at 850 hPa (left) and UPV (right) for the selected EPS members 22 (c and d) and 10 (e and f). Shown are 96 h forecasts for THE850 (c and e) and 168 h PV forecasts of UPV (d and f) together with the corresponding ECMWF operational analysis (a and b).

the other hand EPS member 10 (Figure 8f) predicts the overall upper-tropospheric evolution with its ridge-trough-ridge-trough pattern over the North Atlantic and Europe better, but clearly misses out on the stretching of the PV streamer from Europe into Africa. These examples show how a distinct detail in the +96 h forecasts (here the extension of moist warm air towards the southern tip of Greenland) can decide about the occurrence of a later streamer, despite a worse forecast of the larger-scale UPV fields.

5.3. Statistical Analysis

After the detailed look into one example case, this section continues with a combined analysis of all 75 cases. Geographically fixed mean correlations turned out not to give sufficiently significant results, mainly due to the longitudinal spread of the streamers between 30°W and 30°E (cf. Figure 3c). Instead, shifted composites were generated using the central longitudes of the SRBs described at the end of section 2.3 as a reference. The resulting Figure 9 is constructed in a similar way to Figure 7, although correlations are generally much lower.

Again, we begin the discussion with the evolution at upper levels (top row). Even at +96 h correlations are generally rather low, suggesting limited case-to-case coherence at this stage of the evolution. Highest values of 0.1 are found just to the west of the location of the PV streamer (marked as A) at verification time indicating some tendency towards long-lived and almost stationary systems. The two most conspicuous elements of the correlations during the last three days of the forecast are a coherent wave train in the subtropics (B with dashed line) and a zonally elongated, positively tilted dipole

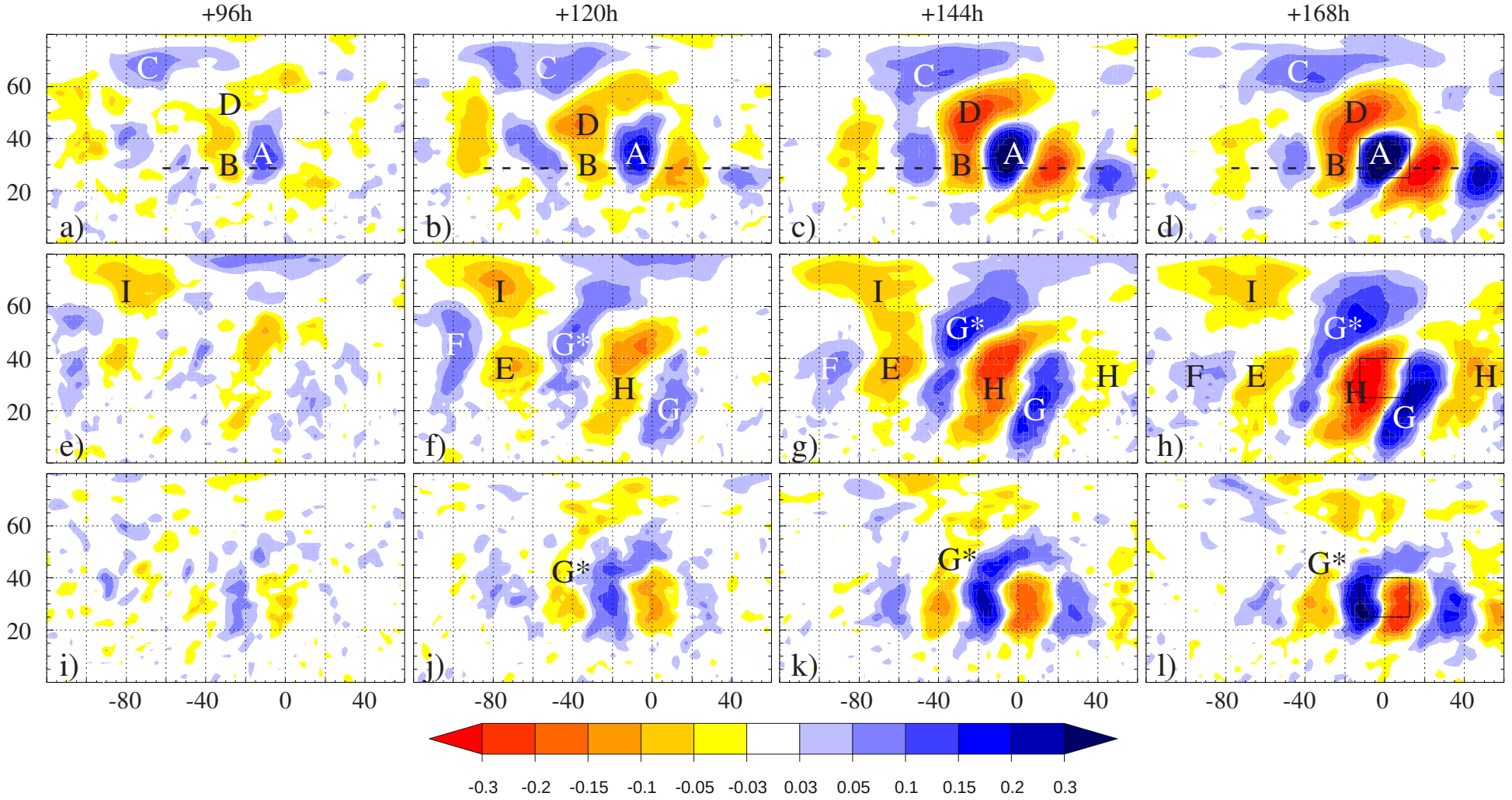

Figure 9. Longitudinally shifted composites of the ensemble correlation coefficients for all 75 PV streamer episodes (in colours; details see text). Correlated atmospheric variables are (i) UPV (top), (ii) equivalent potential temperature at 850 hPa (middle) and (iii) vertical wind at 700 hPa (in pressure coordinates, so negative values correspond to rising) (bottom). Columns vary in forecast time from 96 h (left) to 168 h (right) in steps of 24 h. Note the different contouring with respect to Figure 7.

(C and D) in the extratropics. The former is largely confined to the 20–45°N latitude band with three distinct ridges and troughs, the middle of which is the PV streamer (A). Wavelength is about 50 degrees longitude. While the eastern part is almost stationary, the western part propagates eastward by about 8 degrees longitude leading to some compression of the wave as observed for the case study discussed in section 5.2. The extratropical pattern is dominated by a positive area (C) moving slowly across the North Atlantic (exact location depends on longitude of streamer) and a negative area (D) to the southeast of it, which ultimately merges with the middle ridge (underneath letter B) of the subtropical wave train. This creates the anticyclonic wave breaking that helps to flux additional wave energy into the subtropical wave train, which subsequently strengthens downstream and weakens upstream. There are no clear indications that downstream blocking plays a major role as a precursor of the low-latitude PV streamers.

Reflections of the subtropical wave train are evident in THE850 and w700 (middle and bottom panels in Figure 9) from +120 h onwards. The western part shows a clearly baroclinic structure with subsiding cold/dry air between the ridge and the trough (marked as E) and rising warm/moist air between the trough and the ridge (F). Towards the east, structures become increasingly barotropic with high-THE850 air in the ridges (G/G*) and low-THE850 air in the troughs (H). This behaviour could provide an explanation for the propagation and development in the western part that ultimately lead to a zonal compression of the wavetrain as a whole. It is noteworthy that the THE850 anomalies generally extend farther into the tropics than their counterparts in UPV and w700, indicating some influence of the wave on the thermodynamics of the deeper tropics at this level. In the extratropics, the most coherent feature is the cold/dry anomaly (I) over the northwest of the domain, which is most likely originating over the Canadian Artic. It is rather stationary and remains well west of the UPV signal during the later part of the period, which could be a reflection of cold air damming by Greenland. There is little vertical motion associated with this feature. In term of diabatic modification of UPV by latent heating, the area to the west and north of the forming streamer (H) stands out as an area with widespread high THE850 and rising motion (G*) reaching from the northern tropics beyond the Artic circle. It appears quite likely that this structure helps to reduce UPV in the area of the anticyclonic wave breaking, although the w700 are generally quite weak and are partly collocated with positive UPV anomalies. Particularly at the verification day (Figure 9h) the shape of the positive THE850 correlation with a narrow root at low latitudes and a spreading at the poleward end is reminiscent of a WCB.

6. Conclusions

This study investigated upper-level PV streamers at low latitudes over the Mediterranean Sea/northern Africa during the boreal winter half-year, where/when these events occur most frequently. In total 75 PV streamer episodes were identified objectively using a modified version of the algorithm by Wernli and Sprenger (2007). The main database for this study was operational ensemble predictions from ECMWF for the period 1996–2008. The three main areas of interest for this paper were the quality of the forecasts, the predictability of the atmospheric phenomenon and the identification of dynamical precursors. The main conclusions from this work are:

i As expected, both ensemble spread and RMSE of the ensemble mean calculated with respect to the operational analysis increase monotonically with lead time.

ii The ensemble predictions are generally underdispersive, especially for longer lead times consistent with previous studies for the whole northern hemisphere (Buizza *et al.* 2005). A possible explanation for this could be that forecast errors due to model errors are not represented adequately (Leutbecher and Palmer 2008). However, the

magnitude of the underdispersive behaviour depends on the size of the geographical area used for verification and the parameter used as shown in previous work (e.g. Z500 in the extratropics vs. THE850 in the Tropics). The usage of PV is complicated by the fact that climatological values are generally low in the subtropical troposphere, such that streamers must be regarded as extreme events, which are generally underpredicted as models tend to stay closer to climatology (Toth 1992; Ziehmann 2001).

iii RMSE calculations divided into periods between changes in the operational EPS system showed a general improvement of the EPS over time.

iv PV streamers in the forecasts tend to be shifted to the northeast, suggesting too weak Rossby wave breaking leading to too small meridional extension of the PV streamers.

v Ensemble correlation techniques were used to identify dynamical precursors for low-latitude PV streamers. Results show a key role of interactions between an active wave train in the subtropics and strongly positively tilted PV anomalies in the extratropics, which can lead to anticyclonic wave breaking and an equatorward flux of wave energy. There are some indications that diabatic heating in the area upstream of the PV streamer, where the subtropical and extratropical signals merge, can support the ridge amplification and wave breaking. The connection with upstream latent heating is consistent with previous studies on wave amplification and breaking (Massacand *et al.* 2001; Martius *et al.* 2008). However, some previous studies have also found an importance of downstream blocking for PV streamer development (Altenhoff *et al.* 2008; Meier and Knippertz 2009). The ensemble correlation gives evidence for a ridge downstream of the PV streamer but the signal appears late in the forecast and is not stationary. The subtropical latitudes we concentrated on in this study are not typical for blocking situations and might therefore be dominated by other dynamical factors.

To the best of our knowledge, this is the first time that ensemble correlation techniques are applied for an analysis of dynamical precursors of extreme PV streamers. The fact that each of the real-world streamers is represented by 50 physically plausible realisations from only slightly different initial conditions makes it a powerful analysis tool that is able to account for the fully-nonlinear behaviour of the atmosphere using a state-of-the-art operational system. However, the magnitude of the correlation will always be somewhat sensitive to the spread of the EPS at verification time. In other words, if all ensemble members agree on a certain aspect of the forecast, the signal in the correlation can be expected to be weak. Here, 7-day forecasts are used for verification that usually show significant spread in almost all atmospheric variables. Significantly shorter lead-times are not recommended for this type of analysis.

For possible follow-up studies it is important to keep some of the limitations of this work in mind. One problem clearly is the limited availability of vertical levels in the early part of the EPS database, meaning that only a crude upper-level PV can be calculated. The PV differences used for forecast evaluation can be misleading, as low PV values in the troposphere (0-2 PVU) are compared to the high stratospheric values (2-20 PVU) across the tropopause. Some first thoughts of using a rescaled-PV formulation instead are discussed in Martius *et al.* (2010). In addition, it is not desirable to have a inhomogeneous operational dataset for statistical analyses. It would therefore be interesting to repeat some of the analysis presented here with a hindcast dataset run with a more recent version of the ECMWF EPS and more vertical levels. Moreover, applications of the ensemble correlation techniques to other atmospheric phenomena or geographical regions would be a valuable extension of this work.

Acknowledgement

The authors acknowledge funding for this research from the German Science Foundation (Grant number KN 581/3-1). We would also like to thank the ECMWF for providing the forecast and analysis data, and the German Weather Service and UK Met Office for providing access to the ECMWF database. We are grateful to Heini Wernli for his support with the PV streamer identification and to Doug Parker for suggestions, helpful comments and discussions.

References

Abatzoglou JT, Magnusdottir G. 2004. Nonlinear planetary wave reflection in the troposphere. *Geophysical Research Letters* **31**: L09 101, doi: 10.1029/2004GL019495.

Altenhoff AM, Martius O, Croci-Maspoli M, Schwierz C, Davies HC. 2008. Linkage of atmospheric blocks and synoptic-scale Rossby waves: a climatological analysis. *Tellus Series A* **60**: 1053–1063, doi:10.1111/j.1600-0870.2008.00354.x.

Appenzeller C, Davies H, Norton W. 1996. Fragmentation of stratospheric intrusions. *Journal of Geophysical Research-Atmospheres* **101**(D1): 1435–1456.

Barkan J, Alpert P, Kutiel H, Kishcha P. 2005. Synoptics of dust transportation days from Africa toward Italy and central Europe. *Journal of Geophysical Research-Atmospheres* **110**(D7), doi:10.1029/2004JD005222.

Barkmeijer J, Buizza R, Palmer T. 1999. 3D-Var Hessian singular vectors and their potential use in the ECMWF Ensemble Prediction System. *Quarterly Journal of the Royal Meteorological Society* **125**(558, Part B): 2333–2351.

Berggren R, Bolin B, C-G R. 1949. An aerological study of zonal motion, its perturbations and break-down. *Tellus* **1**: 14–37.

Browning K. 1990. Organization of clouds and precipitation in extratropical cyclones. In: *Extratropical cyclones - The Erik Palmen Memorial Volumen*, Newton, CW and Holopainen, EO (ed). ISBN 1-878220-03-9, pp. 129–153. Palmen memorial symposium on extratropical cyclones, Helsinki, Finland, Aug 29-Sep 02, 1988.

Buizza R, Houtekamer P, Toth Z, Pellerin G, Wei M, Zhu Y. 2005. A comparison of the ECMWF, MSC, and NCEP global ensemble prediction systems. *Monthly Weather Review* **133**(5): 1076–1097.

Buizza R, Petroliagis T, Palmer T, Barkmeijer J, Hamrud M, Hollingsworth A, Simmons A, Wedi N. 1998. Impact of model resolution and ensemble size on the performance of an Ensemble Prediction System. *Quarterly Journal of the Royal Meteorological Society* **124**(550, Part B): 1935–1960.

Carlson TN. 1998. *Mid-latitude weather systems*. American Meteorological Society, Boston.

Davies HC, Schär C, Wernli H. 1991. The palette of fronts and cyclones within a baroclinic wave development. *Journal of Atmospheric Sciences* **48**: 1666–1689.

Eckhardt S, Stohl A, Wernli H, James P, Forster C, Spichtinger N. 2004. A 15-Year climatology of Warm Conveyor Belts. *Journal of Climate* **17**: 218–237, doi:10.1175/1520-0442(2004)017<0218:AYCOWC>2.0.CO;2.

Fehlmann R, Quadri C, Davies HC. 2000. An Alpine rainstorm: Sensitivity to the mesoscale upper-level structure. *Weather and Forecasting* **15**(1): 4–28.

Froehlich L, Knippertz P. 2008. Identification and global climatology of upper-level troughs at low latitudes. *Meteorologische Zeitschrift* **17(5)**: 565–573.

Froude LSR. 2010. TIGGE: Comparison of the prediction of northern hemisphere extratropical cyclones by different Ensemble Prediction Systems. *Weather and Forecasting* **25**(3): 819–836, doi:10.1175/2010WAF2222326.1.

Hawblitzel DP, Zhang F, Meng Z, Davis CA. 2007. Probabilistic evaluation of the dynamics and predictability of the mesoscale convective vortex of 10-13 June 2003. *Monthly Weather Review* **135**(4): 1544–1563, doi:10.1175/MWR3346.1.

Hoinka KP, Davies HC. 2007. Upper-tropospheric flow features and the Alps: An overview. *Quarterly Journal of the Royal Meteorological Society* **133**: 847–865, doi:10.1002/qj.69.

Hoskins BJ, Ambrizzi T. 1993. Rossby wave propagation on a realistic longitudinally varying flow. *Journal of the Atmospheric Sciences* **50**(12): 1661–1671.

Hoskins BJ, McIntyre ME, Robertson AW. 1985. On the use and significance of isentropic potential vorticity maps. *Quarterly Journal of the Royal Meteorological Society* **111**(470): 877–946.

Iskenderian H. 1995. A 10-year climatology of northern-hemisphere tropical cloud plumes and their composite flow patterns. *Journal of Climate* **8**(6): 1630–1637.

Kiladis GN, Weickmann KM. 1992. Extratropical forcing of tropical Pacific convection during winter. *Monthly Weather Review* **120**(9): 1924–1938.

Kiladis GN, Weickmann KM. 1997. Horizontal structure and seasonality of large-scale circulations associated with submonthly tropical convection. *Monthly Weather Review* **125**(9): 1997–2013.

Knippertz P. 2005. Tropical-extratropical interactions associated with an Atlantic tropical plume and subtropical jet streak. *Monthly Weather Review* **133**(9): 2759–2776.

Knippertz P, Fink AH. 2006. Synoptic and dynamic aspects of an extreme springtime Saharan dust outbreak. *Quarterly Journal of the Royal Meteorological Society* **132**(617, Part B): 1153–1177, doi:10.1256/qj.05.109.

Knippertz P, Martin JE. 2005. Tropical plumes and precipitation in subtropical and tropical West Africa. *Quarterly Journal of the Royal Meteorological Society* **131**: 2337–2365.

Knippertz P, Martin JE. 2007. A Pacific moisture conveyor belt and its relationship to a significant precipitation event in the semiarid southwestern United States. *Weather and Forecasting* **22**(1): 125–144, doi:10.1175/WAF963.1.

Leutbecher M, Palmer TN. 2008. Ensemble forecasting. *Journal of Computational Physics* **227**: 3515–3539, doi:10.1016/j.jcp.2007.02.014.

Martius O, Schwierz C, Davies HC. 2008. Far-upstream precursors of heavy precipitation events on the Alpine south-side. *Quarterly Journal of the Royal Meteorological Society* **134**: 417–428, doi:10.1002/qj.229.

Martius O, Schwierz C, Davies HC. 2010. Tropopause-level waveguides. *Journal of Atmospheric Sciences* **67**: 866–879, doi: 10.1175/2009JAS2995.1.

Martius O, Zenklusen E, Schwierz C, Davies HC. 2006. Episodes of alpine heavy precipitation with an overlying elongated stratospheric intrusion: A climatology. *International Journal of Climatology* **26**: 1149–1164, doi:10.1002/joc.1295.

Massacand AC, Wernli H, Davies HC. 1998. Heavy precipitation on the Alpine southside: An upper-level precursor. *Geophysical Research Letters* **25**: 1435–1438, doi:10.1029/98GL50869.

Massacand AC, Wernli H, Davies HC. 2001. Influence of upstream diabatic heating upon an Alpine event of heavy precipitation. *Monthly Weather Review* **129**: 2822–2828, doi:10.1175/1520-0493(2001)129<2822:IOUDHU>2.0.CO;2.

Matsueda M. 2009. Blocking predictability in operational medium-range ensemble forecasts. *SOLA* **5**: 113–116, doi:10.2151/sola.2009-029.

Meier F, Knippertz P. 2009. Dynamics and predictability of a heavy dry-season precipitation event over west africa-sensitivity experiments with a global model. *Monthly Weather Review* **137**(1): 189–206, doi:10.1175/2008MWR2622.1.

Molteni F, Buizza R, Palmer T, Petroliagis T. 1996. The ECMWF Ensemble Prediction System: Methodology and validation. *Quarterly Journal of the Royal Meteorological Society* **122**(529, Part A): 73–119.

Palmer T, Molteni F, Mureau R, Buizza R, Chapelet P, Tribbia J. 1993. 'Ensemble Prediction' pp. 21-66 in Vol. 1 of Proceedings of the ECMWF seminar on validation of models over Europe, 7-11 September 1992 : , ECMWF, Shinfield Park, Reading RG2–9AX, UK.

Pelly JL, Hoskins BJ. 2003. A new perspective on blocking. *Journal of Atmospheric Sciences* **60**: 743–755, doi:10.1175/1520-0469(2003)060<0743:ANPOB>2.0.CO;2.

Postel G, Hitchman M. 1999. A climatology of Rossby wave breaking along the subtropical tropopause. *Journal of the Atmospheric Sciences* **56**(3): 359–373.

Rossby CG. 1959. *The atmosphere and sea in motion*, ch. Current problems in meteorology. Rockefeller Institute Press, New York, pp. 9–50.

Schwierz C, Croci-Maspoli M, Davies HC. 2004a. Perspicacious indicators of atmospheric blocking. *Geophysical Research Letter* **31**: 6125–6128, doi:10.1029/2003GL019341.

Schwierz C, Dirren S, Davies HC. 2004b. Forced waves on a zonally aligned jet stream. *Journal of Atmospheric Sciences* **61**: 73–87.

Slingo A, Ackerman TP, Allan RP, Kassianov EI, McFarlane SA, Robinson GJ, Barnard JC, Miller MA, Harries JE, Russell JE, Dewitte S. 2006. Observations of the impact of a major Saharan dust storm on the atmospheric radiation balance. *Geophysical Research Letters* **33**(24), doi: 10.1029/2006GL027869.

Slingo JM. 1998. Extratropical forcing of tropical convection in a northern winter simulation with the UGAMP GCM. *Quarterly Journal or the Royal Meteorological Society* **124**(545, Part A): 27–51.

Sodemann H, Palmer AS, Schwierz C, Schwikowski M, Wernli H. 2006. The transport history of two Saharan dust events archived in an Alpine ice core. *Atmospheric Chemistry and Physics* **6**: 667–688.

Stoelinga MT. 1996. A potential vorticity-based study of the role of diabatic heating and friction in a numerically simulated baroclinic cyclone. *Monthly Weather Review* **124**: 849–874, doi:10.1175/1520-0493(1996)124<0849:APVBSO>2.0.CO;2.

Thorncroft CD, Flocas HA. 1997. A case study of Saharan cyclogenesis. *Monthly Weather Review* **125**: 1147–1165, doi:10.1175/1520-0493(1997)125<1147:ACSOSC>2.0.CO;2.

Thorncroft CD, Hoskins BJ, McIntyre ME. 1993. Two paradigms of baroclinic-wave life-cycle behaviour. *Quarterly Journal of the Royal Meteorological Society* **119**: 17–55, doi:10.1002/qj.49711950903.

Toth Z. 1992. Quasi-stationary and transient periods in the northern hemisphere circulation series. *Journal of Climate* **5**: 1235–1248, doi: 10.1175/1520-0442(1992)005<1235:QSATPI>2.0.CO;2.

Tripoli GJ, Medaglia CM, Dietrich S, Mugnai A, Panegrossi G, Pinori S, Smith EA. 2005. The 9-10 November 2001 Algerian flood: A numerical study. *Bulletin of the American Meteorological Society* **86**(9): 1229–1235, doi:10.1175/BAMS-86-9-1229.

Waugh DW, Polvani LM. 2000. Climatology of intrusions into the tropical upper troposphere. *Geophysical Research Letters* **27**(23): 3857–3860.

Wernli H, Sprenger M. 2007. Identification and ERA-15 climatology of potential vorticity streamers and cutoffs near the extratropical tropopause. *Journal of the Atmospheric Sciences* **64**(5): 1569–1586, doi:10.1175/JAS3912.1.

Wiegand L, Twitchett A, Schwierz C, Knippertz P. 2011. Heavy precipitation at the Alpine south side and Saharan dust over central Europe: A predictability study using TIGGE. *Weather and Forecasting* **26**: 957–974, doi:10.1175/WAF-D-10-05060.1.

Ziehmann C. 2001. Skill prediction of local weather forecasts based on the ECMWF ensemble. *Nonlinear Processes in Geophysics* **8**: 419–428.